Lattice Boltzmann simulation of weakly ionized plasmas and fluid flows using physical properties of fluids

2009 J. Phys. A: Math. Theor. 42 155501

(http://iopscience.iop.org/1751-8121/42/15/155501)

IOP PUBLISHING JOURNAL OF PHYSICS A: MATHEMATICAL AND THEORETICAL

J. Phys. A: Math. Theor. **42** (2009) 155501 (13pp) doi:10.1088/1751-8113/42/15/155501

Lattice Boltzmann simulation of weakly ionized plasmas and fluid flows using physical properties of fluids

Huayu Li[1] **and Hyungson Ki**[1,2,3]

[1] Department of Mechanical Engineering, Michigan State University, East Lansing, Michigan 48824-1226, USA
[2] School of Mechanical and Advanced Materials Engineering, Ulsan National Institute of Science and Technology, Ulsan, South Korea

E-mail: hski@unist.ac.kr

Received 28 November 2008, in final form 2 February 2009
Published 24 March 2009
Online at stacks.iop.org/JPhysA/42/155501

Abstract
In this paper, we present a lattice Boltzmann method (LBM) to simulate weakly ionized plasmas using physical properties for a wide range of electron number densities. To preserve the convection–diffusion characteristics, this method is based on two scaling rules: (1) the physical viscosity is equal to the lattice viscosity, and (2) the characteristic flow velocity due to the external force should not be altered by the scheme. Although this method has been developed for plasma simulation, it can be applied to other fluid-flow problems. In this study, the present method has been applied to driven cavity flow, Poiseuille flow and the plasma diffusion under an external electric field. It has been shown that this method is applicable to a wide range of electron number densities in the simulation of weakly ionized plasmas.

PACS numbers: 47.11.−j, 52.65.−y, 52.25.Dg

1. Introduction

The lattice Boltzmann method (LBM) has been proved over the past 20 years to be an effective numerical method for simulating fluid flows [1]. Due to its kinetic nature, relatively easy implementation and intrinsic advantage for parallel computation, the LBM has been widely used as an alternative numerical technique not only for ordinary fluid flows [2, 3] but also for complex flow problems, such as nonideal fluid flows [4, 5], multiphase or multicomponent flows [6, 7], flows through porous media [8, 9] and magnetohydrodynamic flows [10–12]. However, despite its close connection with the Boltzmann equation (which is the governing

[3] Author to whom any correspondence should be addressed.

equation for plasma dynamics), only a very small number of LBMs have been developed for plasma simulations [13, 14].

There are intrinsic difficulties in solving plasma problems with the LBM. In the LBM, the lattice kinematic viscosity (which is obtained from the Chapman–Enskog expansion of the lattice Boltzmann equation) is not generally equal to the real kinematic viscosity of the fluid. For some simple flow problems (such as driven cavity flow), the fluid flow is determined solely by a dimensionless number (such as the Reynolds number) and the actual properties of the fluid (in this case kinematic viscosity) do not need to be used as long as the same characteristic dimensionless number (Reynolds number) is maintained. However, in plasma problems, actual physical properties need to be used because a particular dimensionless number does not characterize the flow, and/or the flow is too complicated. In addition, plasmas are driven by the electromagnetic force (Lorentz force), so the full Boltzmann equation with the acceleration term needs to be solved. However, it has not been fully understood whether an additional matching of parameters must be introduced for the acceleration term.

To overcome this problem, Li and Ki [14] introduced a rescaling method for weakly ionized plasmas. With this rescaling scheme, the electrostatic phenomena of weakly ionized helium plasmas with ionization degree of 1–3% and neutral number density of 1×10^{18} m^{-3} were successfully simulated. Numerical tests also showed that this rescaling scheme is valid for neutral number densities roughly between 2×10^{17} m^{-3} and 5×10^{18} m^{-3} with the ionization degree of 1%. However, this is a very narrow range of plasma number densities; in reality, depending on the conditions of plasmas, the number density of plasmas may range from 1×10^{6} m^{-3} to 1×10^{33} m^{-3} and the temperature can be as high as 10^{7} K. The relaxation time as well as the transport properties of the plasma can vary significantly over such a wide range of number densities and temperatures.

This paper presents a new and simpler rescaling scheme that can be used with physical properties of fluids for a wide range of particle number densities in the simulation of weakly ionized plasmas and fluid flows. Weakly ionized plasmas are especially important because plasma-processing technology is vastly used in the fabrication of integrated circuits. Also, plasmas appear in many high-energy manufacturing processes, such as laser welding and pulsed laser deposition. The key idea of this study is to design a scheme in such a way that the kinematic viscosity of the fluid and the characteristic velocity due to the external force are matched in the LBM because, after all, the Boltzmann equation is a convection–diffusion equation. Although this method is developed for plasmas, it can be applied to other flow problems. Also, because this method is based on the authors' previous work [14], this method retains the second-order accuracy of the LBM, which was demonstrated in figure 7 of [14]. In this paper, driven cavity flow, Poiseuille flow and plasma diffusion under externally applied electric fields are simulated to validate the method. Simulation results agree very well with the data from the literature and analytical solutions.

2. Mathematical model

2.1. A brief introduction to the LBM

The continuous Boltzmann equation has the following form:

$$\frac{\partial f}{\partial t} + \mathbf{v} \cdot \nabla_{\mathbf{x}} f + \mathbf{a} \cdot \nabla_{\mathbf{v}} f = Q(f, f'), \tag{1}$$

where $f = f(\mathbf{x}, \mathbf{v}, t)$ is the single particle distribution function in the phase space, $\mathbf{v}$ is the microscopic velocity, $\mathbf{a}$ is the acceleration of fluid particles caused by the external force, and

$Q(f, f')$ is the rate of change of the distribution function due to collisions. If the Bhatnagar–Gross–Krook (BGK) model is used for the collision term, the following equation is obtained:

$$\frac{\partial f}{\partial t} + \mathbf{v} \cdot \nabla_{\mathbf{x}} f + \mathbf{a} \cdot \nabla_{\mathbf{v}} f = -\frac{f - f^{\mathrm{eq}}}{\lambda}. \tag{2}$$

Here, f^{eq} is the equilibrium distribution function, and λ is the relaxation time. Note that the simplification of the collision term by the BGK model is only valid for short-range elastic collisions. In weakly ionized plasmas, since the number density of neutral particles is much greater than that of charged particles, the collisions with neutral particles dominate the process. Thus, we neglect the long-range Coulomb interaction between charged particles in this study. In the standard LBM, equation (2) without the external force term is discretized as [1]

$$f_\alpha(\mathbf{x} + \mathbf{e}_\alpha \Delta t, t + \Delta t) = f_\alpha(\mathbf{x}, t) - \frac{f_\alpha(\mathbf{x}, t) - f_\alpha^{\mathrm{eq}}(\mathbf{x}, t)}{\tau}, \tag{3}$$

where $\mathbf{e}_\alpha$ is the αth component of the discretized microscopic velocity on a lattice, and τ is the dimensionless relaxation time. The desired macroscopic conservation equations, such as the Navier–Stokes equation, can be recovered by the Chapman–Enskog expansion of the lattice Boltzmann equation (equation (3)). The significance of this derivation lies in the fact that some fluid properties, such as kinematic viscosity, can be retrieved from this derivation. The kinematic viscosity obtained by this procedure [2, 15] will be called the lattice viscosity in this paper.

2.2. Determining lattice sound speed and lattice acceleration

The first step of the rescaling procedure is to match kinematic viscosity. In the standard LBM, the lattice viscosity is obtained as follows [2, 15]:

$$\tilde{\nu} = \frac{(\tau - 0.5)}{\sqrt{3}} \tilde{\theta} \Delta x, \tag{4}$$

where Δx is the grid spacing, and $\tilde{\theta}$ is the lattice sound speed. (Here, a tilde is used for lattice parameters.) To preserve the diffusion characteristic of the problem, it is assumed that the lattice kinematic viscosity $\tilde{\nu}$ is equal to the actual kinematic viscosity ν [16]:

$$\nu = \frac{8\theta^2 \lambda}{3\pi}. \tag{5}$$

Here λ is the physical relaxation time, $\lambda = 1/\sigma n \langle v \rangle$ [16] (where σ is the collision cross section, n is the number density of the fluid particles, and $\langle v \rangle$ is the average speed), and θ is the physical sound speed:

$$\theta = \sqrt{\frac{k_B T}{m}}, \tag{6}$$

where k_B is the Boltzmann constant, T is the temperature, and m is the molecular mass of the fluid particle. From equations (4) and (5), the lattice sound speed $\tilde{\theta}$ can be calculated as follows:

$$\tilde{\theta} = \frac{8\theta^2 \lambda}{\sqrt{3}\pi \Delta x (\tau - 0.5)}. \tag{7}$$

From equation (7), we can define the rescaling parameter γ as

$$\gamma \equiv \frac{\theta}{\tilde{\theta}} = \frac{\sqrt{3}\pi \Delta x (\tau - 0.5)}{8\theta\lambda}, \tag{8}$$

following the definition given in the paper by Li and Ki [14]. Then the lattice sound speed is expressed as a function of the rescaling parameter as follows:

$$\tilde{\theta} = \frac{\theta}{\gamma}. \tag{9}$$

Note that the rescaling parameter γ is a function of Δx, λ and θ, and therefore is fixed once the type and condition of fluid (λ and θ) and grid spacing (Δx) are determined. Next, the lattice relaxation time $\tilde{\lambda}$ is determined from the dimensionless relaxation time, $\tilde{\lambda} = \tau \Delta t$, where the time step is $\Delta t = \Delta x/\sqrt{3\tilde{\theta}}$. Using equation (8), the lattice relaxation time $\tilde{\lambda}$ is calculated as follows:

$$\tilde{\lambda} = \frac{8\tau\gamma^2}{3\pi(\tau - 0.5)}\lambda. \tag{10}$$

Secondly, the convective property of the flow when an external force exists must not be altered by the LBM scheme. If the flow is driven by an external force (such as an electromagnetic force), depending on the nature of the force we may need another rescaling to obtain accurate velocity fields. Therefore, we propose the second rescaling rule: the characteristic velocity of the flow should not be changed by the rescaling, i.e.,

$$\mathbf{U}_0 = \tilde{\mathbf{U}}_0, \tag{11}$$

where $\mathbf{U}_0$ is the characteristic velocity of the flow. From this rule, we can obtain the rescaled acceleration $\tilde{\mathbf{a}}$, which we call the lattice acceleration in this paper. Implementation examples will be presented in the results section.

2.3. Choosing dimensionless relaxation time τ

This section provides a guideline to select the dimensionless relaxation time in conjunction with the presented method. In this method, dimensionless relaxation time τ and grid spacing Δx are the two parameters that can be chosen freely. Once Δx is determined, τ can be selected considering the Mach number (Ma) and the Reynolds number (*Re*) of the problem. The following equation is the relationship between the *Re* and Ma obtained from the definition of *Re*:

$$Re = \frac{\sqrt{3}\mathrm{Ma}N}{\tau - 0.5}, \tag{12}$$

where N is the number of grid points along the characteristic length L_0, $\mathrm{Ma} = U_0/\tilde{\theta}$, where U_0 is the characteristic velocity. From equation (12), we obtain

$$\tau = \frac{\sqrt{3}\mathrm{Ma}N}{Re} + 0.5, \tag{13}$$

which must lie in the valid range. Note that according to Hou *et al* [17], there exists a critical value of τ below which simulation results show unphysical patterns or the code diverges even though τ is greater than 0.5. Equation (13) is especially useful when the fluid flow is characterized by the Reynolds number, such as driven cavity flow. Given Ma and *Re*, τ can be determined from equation (13). Also, the Mach number of the problem must be small enough to meet the low Ma requirement. In the mean time, as will be shown in section 3.1, the LBM converges faster with a higher τ.

In cases where *Re* is not important or is hard to define, the definition of Ma can be used to choose τ:

$$\mathrm{Ma} = \frac{\sqrt{3}\pi\Delta x U_0(\tau - 0.5)}{8\theta^2\lambda}, \tag{14}$$

from which the following is obtained:

$$\tau = \frac{8\theta^2 \lambda \mathrm{Ma}}{\sqrt{3}\pi \Delta x U_0} + 0.5. \tag{15}$$

2.4. Implementing the LBM with lattice parameters

The first step in the implementation of the presented scheme is to determine the grid spacing Δx and the dimensionless relaxation time τ (following the method described in section 2.2) and then the rescaling parameter γ according to equation (8) with physical properties of a fluid. Then the lattice sound speed $\tilde{\theta}$ and the lattice acceleration $\tilde{\mathbf{a}}$ are determined from equations (9) and (11), respectively. Once these lattice parameters are obtained, the remaining steps are the same as the standard LBM.

Among various schemes for the discretization of the external force term, He *et al*'s method [18] ($\mathbf{a} \cdot \nabla_{\mathbf{v}} f \approx \mathbf{a} \cdot \nabla_{\mathbf{v}} f^{\mathrm{eq}} = -\frac{\mathbf{a}\cdot(\mathbf{v}-\mathbf{u})}{\theta^2} f^{\mathrm{eq}}$, where $\mathbf{u}$ is the macroscopic velocity) is adopted here. In addition, particle momentum is assumed to be conserved at each collision so that the implicit-time treatment of the external force term can be avoided [18]. Then, the D2Q9 (two-dimensional nine-velocity) lattice Boltzmann equation with an external force is obtained as

$$f_\alpha(\mathbf{x} + \mathbf{e}_\alpha \Delta t, t + \Delta t) = f_\alpha(\mathbf{x}, t) - \frac{f_\alpha(\mathbf{x}, t) - f_\alpha^{\mathrm{eq}}(\mathbf{x}, t)}{\tau} + \frac{\Delta t \tilde{\mathbf{a}} \cdot (\mathbf{e}_\alpha - \mathbf{u})}{\tilde{\theta}^2} f_\alpha^{\mathrm{eq}}(\mathbf{x}, t), \tag{16}$$

where $\mathbf{e}_\alpha$ is the αth component of the discretized microscopic velocity:

$$\mathbf{e}_\alpha = \begin{cases} (0,0) & & \alpha = 0 \\ (\cos\varphi_\alpha, \sin\varphi_\alpha)(\sqrt{3}\tilde{\theta}) & \varphi_\alpha = (\alpha-1)\pi/2 & \alpha = 1,2,3,4 \\ \sqrt{2}(\cos\varphi_\alpha, \sin\varphi_\alpha)(\sqrt{3}\tilde{\theta}) & \varphi_\alpha = (\alpha-5)\pi/2 + \pi/4 & \alpha = 5,6,7,8. \end{cases} \tag{17}$$

The discretized equilibrium distribution function f_α^{eq} is expressed as [19]

$$f_\alpha^{\mathrm{eq}} = \omega_\alpha n \left[1 + \frac{\mathbf{e}_\alpha \cdot \mathbf{u}}{\tilde{\theta}^2} + \frac{(\mathbf{e}_\alpha \cdot \mathbf{u})^2}{2\tilde{\theta}^4} - \frac{\mathbf{u}^2}{2\tilde{\theta}^2} \right], \tag{18}$$

where ω_α is $4/9$ for $\alpha = 0$, $1/9$ for $\alpha = 1, 2, 3, 4$, and $1/36$ for $\alpha = 5, 6, 7, 8$.

The macroscopic quantities can be obtained by taking proper moments of the distribution function with respect to the microscopic velocity. In the LBM, the number density and the macroscopic velocity are calculated as

$$n = \sum_\alpha f_\alpha, \tag{19}$$

$$n\mathbf{u} = \sum_\alpha \mathbf{e}_\alpha f_\alpha. \tag{20}$$

Note that unlike the rescaling method presented in [14], the number density and macroscopic velocity do not need to be further transformed by inversely applying the rescaling rules.

3. Results

3.1. Driven cavity flow: no external force

As the first validation problem, the two-dimensional driven cavity flow [20] is considered. In this problem, no external force appears in the lattice Boltzmann equation, and therefore, only

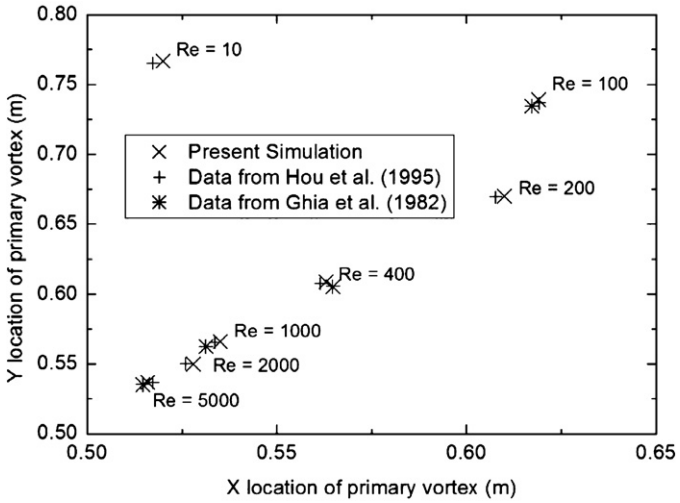

Figure 1. Locations of the primary vortices at different Reynolds numbers.

Table 1. Simulation of driven cavity flow with physical properties of air without the present rescaling method.

	T (K)	p (atm)	ν (m^2 s^{-1})	τ	Ma	Re	Result
Case 1	300	1	1.8245×10^{-5}	0.500 014	1.24×10^{-4}	200	Unstable
Case 2	1500	1×10^{-5}	20.399	7.394	6.22	200	Unstable

Table 2. Simulation of driven cavity flow with physical properties with the presented rescaling method. (Air conditions are given in table 1).

	Re	Ma	τ	γ	No of iterations
Case 1	200	9.021×10^{-2}	0.6	7252.43	203 80
Case 2	200	9.021×10^{-2}	0.6	1.45×10^{-2}	20 380

the first rescaling rule is employed to obtain the lattice sound speed and the acceleration is not rescaled. The governing equation for this flow is equation (16) without the external force term. The cavity is 1 m $\times$ 1 m in size and a 128 $\times$ 128 grid is used. We terminated the computation when the maximum relative error of the distribution function between two successive time steps is less than 1×10^{-6}.

To show the capabilities of the rescaling scheme, driven cavity flow is simulated for two different conditions of air. Table 1 shows the properties of air, and Re is selected to be 200 for both cases. As expected, the LBM fails in both cases without the rescaling. However, both cases are simulated correctly by using the rescaling scheme. Table 2 lists the parameters used in the simulations with the rescaling and the numbers of iterations until convergence. Note that Ma and τ are in the reasonable range.

Next, we simulate the driven cavity flow problem at several different Re using the properties used in case 1 (in table 1) with the rescaling. The main simulation parameters are listed in table 3. Figure 1 presents the locations of the primary vortices at different Re, and figure 2 shows the velocity profiles along the central lines at two different Reynolds numbers

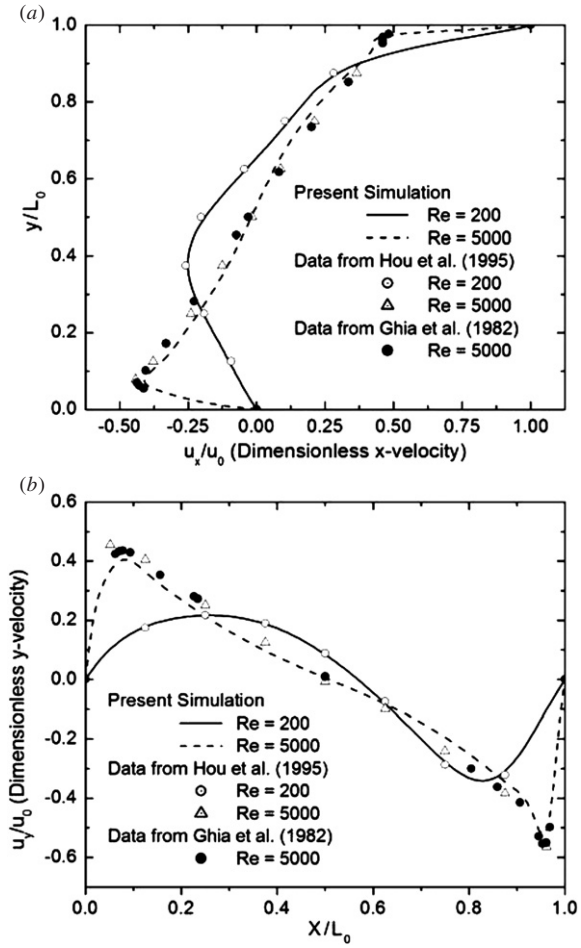

Figure 2. Velocity profiles along the central lines of the computational domain. (*a*) Dimensionless *x*-velocity (*b*) dimensionless *y*-velocity.

(200, 5000). A primary vortex is the largest vortex located near the center and is directly created by the motion of the lid; in contrast, secondary vortices are located at the corners and are driven by the primary vortex. As seen, flow patterns are in good agreement with the results reported in [17] and [20]. In figure 2, we can see that the error at $Re = 5000$ is relatively large, which can be explained by the high Ma (Ma $= 0.564$) resulting from $Re = 5000$ and $\tau = 0.525$ as shown in table 3. According to equation (12), there are two ways to reduce the Ma when *Re* is large. One way is to decrease τ. But unfortunately, there is a lower limit of τ due to the nature of the LBM. The closer the value of τ is to 0.5, the more likely the code will be unstable. The other way is to increase the grid density for the simulation. This is the most straightforward way to solve this problem in a moderate range of *Re* but, of course, will increase the computational expense. Besides these two methods, there is another way to reduce Ma, i.e., the use of an interpolation scheme after the collision-streaming steps in the LBM [21].

Table 3. Simulation parameters for air at 300 K and 1 atm (case 1).

Re	Ma	τ	γ
100	0.1	0.72	15 955.35
200	0.0902	0.6	7252.43
500	0.113	0.55	3626.22
1000	0.113	0.525	1813.11
2000	0.225	0.525	1813.11
5000	0.564	0.525	1813.11

3.2. Poiseuille flow

As the second example, the Poiseuille flow is simulated, where the constant pressure gradient $\mathrm{d}p/\mathrm{d}x$ is treated in the acceleration term of the lattice Boltzmann equation, $\mathbf{a} = \left[-\frac{1}{\rho}\frac{\mathrm{d}p}{\mathrm{d}x}, 0\right]$, and therefore, both the rescaling rules must be applied. The analytical solution can be easily obtained:

$$\mathbf{v} = \left[-\frac{1}{\rho\nu}\frac{\mathrm{d}p}{\mathrm{d}x} y\left(H - \frac{y}{2}\right), 0\right]. \tag{21}$$

The walls are located at $y = 0$ and $y = 2H$, and ρ is the density of the fluid. The choice of the lattice sound speed by the first rule is explained in section 2.1. To apply the second rule, the characteristic velocity must be identified, which is the maximum velocity along the centerline and can be obtained from equation (21) as follows:

$$\mathbf{U}_0 = \left[-\frac{H^2}{2\rho\nu}\frac{\mathrm{d}p}{\mathrm{d}x}, 0\right] = \frac{\mathbf{a}H^2}{2\nu}. \tag{22}$$

From the second rule, this velocity should not be changed by the rescaling, so we have

$$\frac{\mathbf{a}H^2}{2\nu} = \frac{\tilde{\mathbf{a}}H^2}{2\tilde{\nu}}. \tag{23}$$

Since $\tilde{\nu} = \nu$ from the first rescaling rule, we can find that $\tilde{\mathbf{a}} = \mathbf{a}$, which means for Poiseuille flow, no rescaling is required for the acceleration term.

For the numerical test, air at 300 K and 1 atm is considered and $8.898 \times 10^{-5}\,\mathrm{N\,m^{-3}}$ is used for $\mathrm{d}p/\mathrm{d}x$. A 1 m $\times$ 0.125 m domain is used ($H = 0.0625$ m) and the grid density is 256×32. The dimensionless relaxation time is selected as $\tau = 0.6$. Figure 3 shows the simulated steady-state velocity profile with the analytical solution (equation (21)). Apparently, the simulation result obtained by the rescaling scheme agrees very well with the analytical solution.

3.3. Weakly ionized plasmas under external electric fields

The present rescaling scheme can be applied to weakly ionized isothermal plasmas. In fact, the numerical method used in this section is the same as that proposed in [14] except the rescaling scheme part, so only a brief description about the method will be given in this paper. Unlike the method given in [14], the current scheme rescales only $\tilde{\theta}$ and $\tilde{\mathbf{a}}$, and dimensionless relaxation time τ is chosen following the guidelines presented in section 2.2. In addition, no inverse rescaling is needed to obtain density and velocity. This method extends the capabilities of the previous scheme [14] to a much wider range of plasma conditions.

In this paper, we simulate the electron diffusion problem under an externally applied electric field by neglecting the internally generated electric field because, in this case,

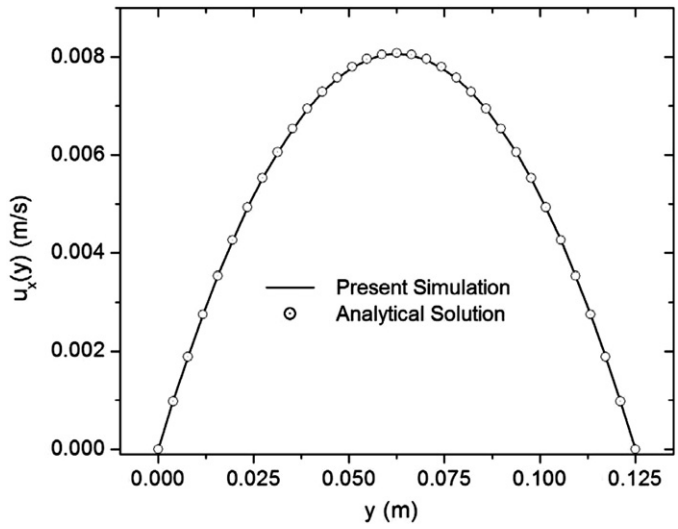

Figure 3. Steady-state velocity profile of the Poiseuille flow.

the analytical solution is available. Inclusion of the internally generated electric field is straightforward and will not be considered here. The details on the problem, such as domain size and grid density, can be found in [14]. For electrostatic plasmas, the acceleration due to the Coulomb force is $\mathbf{a}_s = q_s\mathbf{E}/m_s$, where $\mathbf{E}$ is the electric field, q_s is the charge of species s ($s = e, i, n$), and m_s is the mass of species s.

If the initial electron distribution is Gaussian and the maximum degree of ionization is 1%, the temporal and spatial distribution of the electron number density is calculated analytically as

$$n_e^A(x, y, t) = \frac{0.01 n_{n0}}{(1 + t/t_0)} \exp\left[-\frac{(x - x_c - v_d t)^2 + (y - y_c)^2}{r^2(1 + t/t_0)}\right], \tag{24}$$

where $t_0 = r^2/4D$, $r = 0.290$ mm, (x_c, y_c) represents the center point of the initial Gaussian distribution of electrons, and the diffusivity D can be calculated from [16]

$$D = \frac{\langle v_e\rangle^2 \lambda_{en}}{3}, \tag{25}$$

where $\langle v_e\rangle = \sqrt{8/\pi}\theta_e$ and $\theta_e = \sqrt{k_B T_e/m_e}$ is the electron sound speed, and $\lambda_{en} = 1/\sigma_{en} n_n \langle v_e\rangle$ is the relaxation time due to the collisions between electrons and neutrals where σ_{en} is the collision cross section. In equation (24), v_d is the magnitude of the electron drift velocity $\mathbf{v}_d$ due to the external electric field, which is calculated as follows [22]:

$$\mathbf{v}_d = -\frac{e\mathbf{E}_0}{m_e}\lambda_{en} = \mathbf{a}_e\lambda_{en}. \tag{26}$$

In this problem, the second rule must be applied to rescale the acceleration term. Because the drift velocity is the characteristic velocity due to the electric field in this case, i.e., $\mathbf{U}_0 = \mathbf{v}_d$, from equation (11) and equation (26) the following equation can be obtained:

$$\mathbf{a}_e\lambda_{en} = \tilde{\mathbf{a}}_e\tilde{\lambda}_{en}, \tag{27}$$

from which the acceleration due to the external force is rescaled as follows:

$$\tilde{\mathbf{a}}_e = \frac{3\pi(\tau - 0.5)}{8\tau\gamma^2}\mathbf{a}_e, \tag{28}$$

Table 4. Simulation parameters used for the plasma diffusion problem.

n_{n0} (m^{-3})	T_e (eV)	τ	γ	E_0 (V m^{-1})	Error
1×10^{16}	0.7005	1.5	9.686×10^{-9}	14 226.72	1.494×10^{-6}
1×10^{18}	0.8008	1.5	9.686×10^{-7}	16 270.90	1.495×10^{-6}
1×10^{20}	0.9343	1.5	9.686×10^{-5}	18 975.84	1.494×10^{-6}
1×10^{22}	1.1186	1.5	9.686×10^{-3}	22 731.20	1.495×10^{-6}
1×10^{24}	1.3891	1.5	0.9686	28 288.26	1.498×10^{-6}
1×10^{26}	1.820	1.5	96.86	58 822.30	2.343×10^{-6}

where equation (10) is used to replace $\tilde{\lambda}_{en}$. Note that this time the lattice acceleration is different from the physical acceleration because unlike the Poiseuille flow case the characteristic velocity is a function of the relaxation time (see equation (26)).

Assuming that the plasma is singly ionized, the lattice Boltzmann equations are written separately for electrons, ions and neutrals as follows [14]:

$$f_e^\alpha\left(\mathbf{x}+\mathbf{e}_e^\alpha\Delta t, t+\Delta t\right) = f_e^\alpha(\mathbf{x},t) - \frac{1}{\tau_{en}}\left[f_e^\alpha(\mathbf{x},t) - f_{en}^{\mathrm{eq},\alpha}(\mathbf{x},t)\right] + \frac{\Delta t\tilde{\mathbf{a}}_e\cdot\left(\mathbf{e}_e^\alpha-\mathbf{u}_e\right)}{\tilde{\theta}_e^2} f_e^{\mathrm{eq},\alpha}, \tag{29}$$

$$f_i^\alpha\left(\mathbf{x}+\mathbf{e}_i^\alpha\Delta t, t+\Delta t\right) = f_i^\alpha(\mathbf{x},t) - \frac{1}{\tau_{in}}\left[f_i^\alpha(\mathbf{x},t) - f_{in}^{\mathrm{eq},\alpha}(\mathbf{x},t)\right] + \frac{\Delta t\tilde{\mathbf{a}}_i\cdot\left(\mathbf{e}_i^\alpha-\mathbf{u}_i\right)}{\tilde{\theta}_i^2} f_i^{\mathrm{eq},\alpha}, \tag{30}$$

$$f_n^\alpha\left(\mathbf{x}+\mathbf{e}_n^\alpha\Delta t, t+\Delta t\right) = f_n^\alpha(\mathbf{x},t) - \frac{1}{\tau_{nn}}\left[f_n^\alpha(\mathbf{x},t) - f_{nn}^{\mathrm{eq},\alpha}(\mathbf{x},t)\right], \tag{31}$$

where τ_{sn} is the dimensionless relaxation time for the collisions between species s and neutrals, $\tilde{\theta}_s$ is the lattice sound speed of species s, and $f_{sn}^{\mathrm{eq},\alpha}$ is the discretized equilibrium distribution function for the collisions between species s and neutrals:

$$f_{sn}^{\mathrm{eq},\alpha} = \omega_\alpha n_s\left[1 + \frac{\mathbf{e}_s^\alpha\cdot\mathbf{u}_{sn}}{\tilde{\theta}_s^2} + \frac{\left(\mathbf{e}_s^\alpha\cdot\mathbf{u}_{sn}\right)^2}{2\tilde{\theta}_s^4} - \frac{\mathbf{u}_{sn}^2}{2\tilde{\theta}_s^2}\right]. \tag{32}$$

Here, n_s is the number density of species s, and $\mathbf{u}_{sn}$ is the barycentric velocity of the binary collision with the neutral particles:

$$\mathbf{u}_{sn} = \frac{\rho_s\mathbf{u}_s + \rho_n\mathbf{u}_n}{\rho_s+\rho_n}, \tag{33}$$

where $\mathbf{u}_s$ and ρ_s are macroscopic velocity and mass density of species s, respectively. Note that even with only a 1% ionization degree, collisions with charged particles may not be negligible because the collision cross sections for the collisions between charged particles could be much larger than those for the collisions with neutral particles [23–25]. In such a case, equations (29) and (30) need to be modified accordingly. Because this paper is focused on the LBM for the Boltzmann equation with a BGK collision term, those possibilities will not be considered in this study.

Table 4 lists initial neutral number density (n_{n0}), electron temperature (T_e) and other parameters used for the simulation. Here, T_e is obtained from the Saha equation [26] corresponding to the 1% ionization degree and the electric field $\mathbf{E}_0$ directs from left to right. The dimensionless relaxation time τ is set to 1.5 for all the calculations.

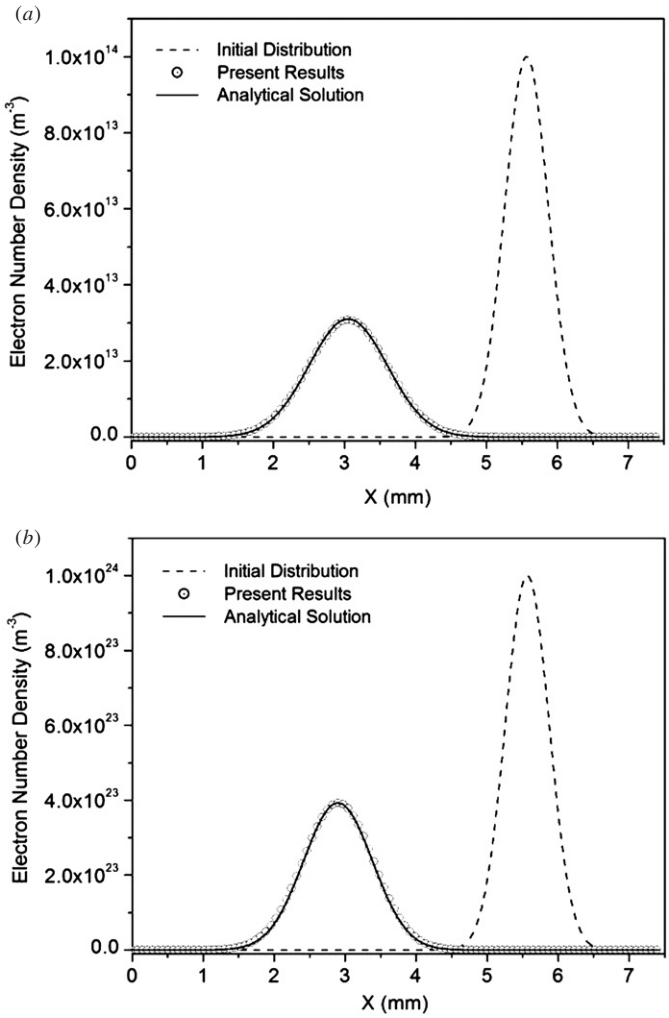

Figure 4. Electron number density distributions with the analytical solutions: (*a*) $n_{n0} = 1 \times 10^{16}\,\mathrm{m}^{-3}$ at $t = 3.36 \times 10^{-16}$ s, (*b*) $n_{n0} = 1 \times 10^{26}\,\mathrm{m}^{-3}$ at $t = 1.433 \times 10^{-6}$ s.

In this paper, a wide range of neutral number density (from 1×10^{16} to $1 \times 10^{26}\,\mathrm{m}^{-3}$) is considered. In figure 4, electron number density distributions at later times are plotted together with the analytical solution (equation (24)) for two different initial neutral density values (1×10^{16} and $1 \times 10^{26}\,\mathrm{m}^{-3}$). The simulation errors for six different initial number density values are listed in table 4 using the following formula [14]:

$$\text{error} = \sqrt{\sum_{i,j}\left[\frac{n_e^{\mathrm{LB}}(i,\,j,\,t) - n_e^{A}(x_i,\,y_j,\,t)}{n_e^{A}(i,\,j,\,t)}\right]^2 \Big/ mn}, \tag{34}$$

where m and n are numbers of grid points in x and y directions, respectively, $n_e^{\mathrm{LB}}(i,\,j,\,t)$ is the electron number density at node point $(i,\,j)$ obtained by the simulation, and $n_e^{A}(x_i,\,y_j,\,t)$ is the electron number density at the corresponding space point by equation (24). As clearly shown

from figure 4 and table 4, the present rescaling scheme gives good results for the electron diffusion problem for a wide range of electron number density.

4. Conclusion

In summary, a rescaling scheme has been proposed by which the LBM with an external force term can be used with physical properties of fluids. This scheme only rescales the sound speed and the acceleration term due to external forces based on the following two rules: (1) the physical viscosity is equal to the lattice viscosity, and (2) the characteristic velocity due to the external force is not affected by the rescaling scheme. For validation purposes, the present scheme has been applied to the lid-driven cavity flow (where no external force is involved), the Poiseuille flow (where acceleration is not changed by the rescaling) and the plasma diffusion problem due to an externally applied electric field (where the acceleration is changed by the rescaling). Simulation results agree well with the data available in the literature and the analytical solutions to the electron diffusion problem. In particular, this scheme can be applied to a wide range of number densities in plasma simulations.

Acknowledgment

This research was supported, in part, by the US National Science Foundation (grant no 0425217).

References

[1] Chen S and Doolen G D 1998 Lattice Boltzmann method for fluid flows *Annu. Rev. Fluid Mech.* **30** 329–64
[2] He X Y and Luo L S 1997 Lattice Boltzmann model for the incompressible Navier–Stokes equation *J. Stat. Phys.* **88** 927–44
[3] Yu H D and Zhao K H 1999 Lattice Boltzmann model for compressible flow simulation *Acta Phys. Sin.* **48** 1470–6
[4] Luo L S 2000 Theory of the lattice Boltzmann method: lattice Boltzmann models for nonideal gases *Phys. Rev.* E **62** 4982–96
[5] Gonnella G, Lamura A and Sofonea V 2007 Lattice Boltzmann simulation of thermal nonideal fluids *Phys. Rev.* E **76** 036703
[6] Xu A G 2005 Finite-difference lattice-Boltzmann methods for binary fluids *Phys. Rev.* E **71** 066706
[7] Shan X W and Chen H D 1993 Lattice Boltzmann model for simulating flows with multiple phases and components *Phys. Rev.* E **47** 1815–9
[8] Seta T, Takegoshi E and Okui K 2006 Lattice Boltzmann simulation of natural convection in porous media *Math. Comput. Simul.* **72** 195–200
[9] Pan C X, Luo L S and Miller C T 2006 An evaluation of lattice Boltzmann schemes for porous medium flow simulation *Comput. Fluids* **35** 898–909
[10] Martinez D O, Chen S Y and Matthaeus W H 1994 Lattice Boltzmann magnetohydrodynamics *Phys. Plasmas* **1** 1850–67
[11] Schaffenberger W and Hanslmeier A 2002 Two-dimensional lattice Boltzmann model for magnetohydrodynamics *Phys. Rev. E* **66** 046702
[12] Li H Y and Ki H 2008 Simulation of MHD flows using a hybrid lattice-Boltzmann finite-difference method *Commun. Comput. Phys.* **4** 337–49
[13] Macnab A I D *et al* 2006 Non-local closure and parallel performance of lattice Boltzmann models for some plasma physics problems *Phys. Stat. Mech. Appl.* **362** 48–56
[14] Li H Y and Ki H 2007 Lattice Boltzmann method for weakly ionized isothermal plasmas *Phys. Rev.* E **76** 066707
[15] Yu D Z *et al* 2003 Viscous flow computations with the method of lattice Boltzmann equation *Prog. Aerosp. Sci.* **39** 329–67
[16] Gombosi T I 1994 *Gaskinetic Theory Cambridge Atmospheric and Space Science Series, (Cambridge, England)* vol 14 (New York: Cambridge University Press) p 297

[17] Hou S L *et al* 1995 Simulation of cavity flow by the lattice Boltzmann method *J. Comput. Phys.* **118** 329–47
[18] He X Y, Shan X W and Doolen G D 1998 Discrete Boltzmann equation model for nonideal gases *Phys. Rev.* E **57** R13–6
[19] He X Y and Luo L S 1997 Theory of the lattice Boltzmann method: from the Boltzmann equation to the lattice Boltzmann equation *Phys. Rev.* E **56** 6811–7
[20] Ghia U, Ghia K N and Shin C T 1982 High-re solutions for incompressible-flow using the Navier Stokes equations and a multigrid method *J. Comput. Phys.* **48** 387–411
[21] He X Y and Doolen G 1997 Lattice Boltzmann method on curvilinear coordinates system: flow around a circular cylinder *J. Comput. Phys.* **134** 306–15
[22] Makabe T and Petroviac Z 2006 Plasma electronics: applications in microelectronic device fabrication *Series in Plasma Physics* (New York: Taylor & Francis) p 339
[23] Vranjes J *et al* 2008 Energy flux of Alfven waves in weakly ionized plasma *Astron. Astrophys.* **478** 553–8
[24] Vranjes J and Poedts S 2008 Note on the role of friction-induced momentum conservation in the collisional drift wave instability *Phys. Plasmas* **15** 034504
[25] Vranjes J *et al* 2008 Collisional energy transfer in two-component plasmas *Phys. Plasmas* **15** 092197
[26] Bittencourt J A 2004 *Fundamentals of Plasma Physics* vol 23 3rd edn (New York: Springer) p 678